



## 1 **Modeling of terrain effect in magnetotelluric data from Garhwal Himalaya Region**

2 Suman Saini<sup>1\*</sup>, Deepak Kumar Tyagi<sup>2</sup>, Sushil kumar<sup>3</sup>, Rajeev Sehrawat<sup>1\*\*</sup>

3 <sup>1</sup>Department of Physics, M. M. Engineering College, Maharishi Markandeshwar (Deemed to be)  
4 University, Mullana-Ambala, Haryana, India 133207

5 Corresponding Author- Rajeev Sehrawat<sup>1\*\*</sup>

6 \*\*Email: [rajeev.sehrawat@mmumullana.org](mailto:rajeev.sehrawat@mmumullana.org)

7 \*Email: [sumanabcd12@gmail.com](mailto:sumanabcd12@gmail.com)

8 <sup>2</sup>Department of Physics, Krishnan College of Science and IT, M.J.P. Rohilkhand University, Bijnor,  
9 Uttar Pradesh, India-246701

10 <sup>3</sup>Department of Geophysics, Kurukshetra University, Kurukshetra, India-136119

### 11 **ABSTRACT**

12 The magnetotelluric method (MT) is one of the most effective geophysical techniques for studying the  
13 deep structure of the Earth's crust, particularly in steep terrain like the Garhwal Himalaya region. The  
14 MT responses are distorted as a result of the undulated/rugged terrain. Such responses, if not  
15 corrected, can lead to a misinterpretation of MT data for the geoelectrical structures. In this research  
16 paper, two different correction procedures were used to compute the topography distortion for the  
17 synthetic model of Garhwal Himalaya region from Roorkee to Gangotri section. A finite difference  
18 algorithm was used to compute MT responses (apparent resistivity and phase) for the irregular terrain.  
19 The accuracy of the terrain correction procedures was checked on results published in the literature on  
20 different topography models at various periods. The relative errors between flat earth response (FER)  
21 and two terrain correction procedures (TCR1 and TCR2) were calculated and were very less or almost  
22 zero for most of the sites along the Roorkee to Gangotri profile except at the foothill where the error  
23 was high at lower periods. The similar topography response, terrain corrected responses TCR1 and



24 TCR2 responses concluded that there is no need for topography correction along Roorkee-Gangotri  
25 Profile because the slope angle is less than one degree.

26 **Keywords:** Magnetotelluric, Topography correction procedures, Himalaya region

## 27 1. INTRODUCTION

28 The magnetotelluric (MT) method was first explored by Tikhonov (1950) and Cagniard (1953) and  
29 was used to analyse the time-varying measured components of earth's natural time-varying electric  
30 and magnetic fields to determine the interior of the earth. MT technique has been successfully used to  
31 explore a variety of earth resources, including oil, gas, mineral, and geothermal energy (Zhang et al.,  
32 2014; Patro et al., 2017; Mohan et al., 2017). The MT method is effective for analysing deep crystal  
33 structures in challenging undulating terrains, such as the Himalayan region as compared to the seismic  
34 method (Tyagi , 2007; Israil et al., 2008, 2016; Pavan Kumar et al., 2014; Patro and Harinarayana,  
35 2009; Kumar et al., 2018, 2022; Xiong-Bin, 2020; Dharmendra Kumar et al., 2021; Konda et al.,  
36 2023). Topography affects both the electric field and magnetic field components due to undulating  
37 topographical features like hills and valleys, which distort the current lines (Wannamaker et al., 1986;  
38 Michel Choutraus et al., 1988; Changhong et al., 2018; Kumar et al., 2018, 2022). Therefore, the MT  
39 response functions impedance and apparent resistivity get distorted when the MT sites are on or near  
40 the top of the hill or close to the valley.

41 Analytical and numerical techniques have been used to measure the topography distortion effect from  
42 MT data. Analytical techniques based on conformal mapping were used by Thayer (1975),  
43 Harinarayana and Sarma (1982). Numerical techniques have been used for different types of terrain  
44 geometrics to remove topography effects from the data (Wannamaker et al., 1986; Michel and  
45 Bouchard, 1988; WescotHessler, 1962; Faradzhev, 1972). The distortions in MT data due to



46 topography and near-surface inhomogeneities have been observed by many researchers (Jiracek, 1990;  
47 Vozoff, 1991). The distortion tensor stripping-off technique has been used to reduce the topographic  
48 effect and to remove the distortion due to the near-surface heterogeneity (Larsen, 1971). The  
49 analogue, analytic, and numerical solution methods were used to study the analogue model (Wescott  
50 and Hessler, 1962; Faradzhev et al., 1972). Various two-dimensional (2D) numerical techniques have  
51 been used for the numerical treatment of the topographic effects like networking analogy (Ku et al.,  
52 1973; NgCo, 1980) and Rayleigh scattering numerical modeling techniques (Jiracek Redding and  
53 Kojima, 1989) and finite element method (Wannamaker Stodt and Rijo, 1986; Frankle et al., 2007).  
54 In 2D, the topography effect is galvanic in Transverse Magnetic (TM) mode and inductive in  
55 Transverse Electric (TE) mode, hence more distortion in TM mode than TE mode (Gurer and Ilikisik,  
56 1997; Kumar et al., 2014; Kumar et al., 2018, 22).

57 In this study, modified 2D forward and inversion modeling code EM2INV (Rastogi, 1997) based on  
58 the finite difference method were used to compute MT forward modeling responses over flat earth and  
59 topographic surface. Two different terrain correction procedures have been used in this study, first  
60 correction procedure was adopted from Chouteau and Bouchard (1988) and the second was adopted  
61 from Nam et al., (2008) to compute the topography distortion for the synthetic model of Garhwal  
62 Himalayan region (Roorkee-Gangotri section). The results of both terrain correction procedures have  
63 been compared to the model used by Chouteau and Bouchard (1988).

## 64 **2. METHODOLOGY**

65 The topography correction to the MT data has been applied by two different techniques. The first  
66 technique was introduced by Chouteau and Bouchard (1988) to estimate the distortion tensor and  
67 correction of MT data before inversion of MT data. In the second approach, the distortion tensor



68 stripping-off technique was used to remove the distortion from the MT data (Larsen, 1977 and Nam et  
69 al., 2008). Two correction procedures first adopted by Chouteau and Bouchard (1988) and second by  
70 Nam et al., (2008) were used to correct the MT data.

### 71 **2.1 Terrain correction procedure 1 (TCPI):-**

72 The computational algorithm for 2D forward modeling has been used to account for irregular terrain.  
73 The distortion tensor for the topographic effect was calculated using the technique adopted by  
74 Chouteau and Bouchard (1988). Based on the assumption that the topography distorted subsurface  
75 field can be approximated by multiplying the distortion tensor by the subsurface field for a flat earth  
76 given by:

$$77 \quad \widetilde{E}_D = D\widetilde{E}_N \quad (1)$$

78 Where  $\widetilde{E}_D$  and  $\widetilde{E}_N$  are the distorted and normal electric field matrices with elements  $E(f, r)_D$  and  
79  $E(f, r)_N$  respectively.  $\widetilde{D}$  is the distortion tensor with elements  $D(f, r)$ , where  $f$  is frequency and  $r$  is  
80 the measuring site position. In case of 2D problem in H- polarization and x-axis is the direction of  
81 strike, equation (1) can be written as

$$82 \quad E_{xD}(f, r) = D_{XX}(f, r)E_{xN}(f, r) \quad (2)$$

83 The impedance tensor can be calculated by dividing equation (2) with magnetic field  $H_y$ .

$$84 \quad Z_D(f, x) = D(f, x)Z_N(f, x) \quad (3)$$

85 Where  $Z_N(f, x)$  and  $Z_D(f, x)$  are respectively the normal (flat earth) impedance and distortion  
86 impedance. Distortion coefficients  $D(f, x)$  are complex coefficients that should just reflect  
87 topography effect. The distortion coefficients are calculated by normalizing the impedances  $Z_t(f, x)$



88 computed over topographic model above a homogeneous medium with the half-space impedance.

89 Thus, the corrected impedance over flat earth can be calculated by taking the following ratio of the

90 observed impedances,  $Z_D(f, x)$ , over irregular topography to the distortion coefficients  $D(f, x)$ :

$$91 \quad Z_C(f, x) = Z_D(f, x)/D(f, x) \quad (4)$$

92 Where  $Z_C(f, x)$  is terrain-corrected impedance.

### 93 **2.2 Terrain correction procedure 2 (TCP2):-**

94 In this correction procedure, the MT data was corrected using the technique adopted by Nam et al.,

95 (2008). Larsen (1977) introduced the distortion tensor stripping-off technique, in which the

96 undistorted impedance tensor can be calculated using a linear relationship between the distorted and

97 undistorted impedance tensor, and topography distorted MT data can be corrected by computing the

98 distortion tensor. The undistorted impedance tensor is linearly related to the distorted impedance

99 tensor as:

$$100 \quad Z^D = D^Z \cdot Z^U \quad (5)$$

101 Where  $Z^D$  is the distortion impedance tensor,  $D^Z$  is distortion tensor and  $Z^U$  is the undistorted

102 impedance tensor respectively. The distortion tensor can be calculated from the relation between the

103 impedance tensor for a homogeneous medium with topography earth surface ( $Z^t$ ), and that with the

104 flat earth surface ( $Z^h$ ) as

$$105 \quad Z^t = D^Z \cdot Z^h \quad (6)$$

106 In case of 2D,  $Z_{xx}^h = Z_{yy}^h = (0, 0)$  and  $Z_{xy}^h \neq -Z_{yx}^h$ , the inhomogeneous earth distortion tensor,

107 equations (5) and (6) can be rewritten in matrix form as



$$108 \quad \begin{bmatrix} 0 & Z_{xy}^D \\ Z_{yx}^D & 0 \end{bmatrix} \begin{bmatrix} 0 & D_{xy}^Z \\ D_{yx}^Z & 0 \end{bmatrix} \begin{bmatrix} 0 & Z_{xy}^U \\ Z_{yx}^U & 0 \end{bmatrix} \quad (7)$$

109 and

$$110 \quad \begin{bmatrix} 0 & Z_{xy}^t \\ Z_{yx}^t & 0 \end{bmatrix} = \begin{bmatrix} 0 & D_{xy}^Z \\ D_{yx}^Z & 0 \end{bmatrix} \begin{bmatrix} 0 & Z_{xy}^h \\ Z_{yx}^h & 0 \end{bmatrix} \quad (8)$$

111 So

$$112 \quad \begin{bmatrix} 0 & D_{xy}^Z \\ D_{yx}^Z & 0 \end{bmatrix} = \begin{bmatrix} 0 & Z_{xy}^t \\ Z_{yx}^t & 0 \end{bmatrix} \begin{bmatrix} 0 & Z_{xy}^h \\ Z_{yx}^h & 0 \end{bmatrix}^{-1} \quad (9)$$

$$113 \quad \begin{bmatrix} 0 & D_{xy}^Z \\ D_{yx}^Z & 0 \end{bmatrix} = \begin{bmatrix} (Z_{xy}^t)/(Z_{xy}^h) & 0 \\ 0 & (-Z_{yx}^t)/(Z_{yx}^h) \end{bmatrix} \quad (10)$$

114 Substituting equation (10) in equation (7)

$$115 \quad \begin{bmatrix} 0 & Z_{xy}^D \\ Z_{yx}^D & 0 \end{bmatrix} = \begin{bmatrix} (Z_{xy}^t)/(Z_{xy}^h) & 0 \\ 0 & (-Z_{yx}^t)/(Z_{yx}^h) \end{bmatrix} \begin{bmatrix} 0 & Z_{xy}^U \\ Z_{yx}^U & 0 \end{bmatrix} \quad (11)$$

116 The undistorted or corrected impedance tensor component can be obtained as

117 So

$$118 \quad Z_{xy}^U = (Z_{xy}^h Z_{xy}^D)/(Z_{xy}^t) \quad (12)$$

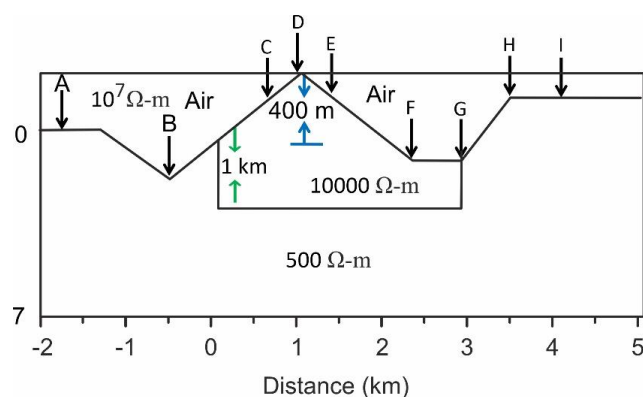
$$119 \quad Z_{yx}^U = (Z_{yx}^h Z_{yx}^D)/(Z_{yx}^t) \quad (13)$$

### 120 **3. TESTING THE CORRECTION PROCEDURES:**

121 In this study, we replicated the model of Chouteau and Bouchard (1988). A 2D topographic  
122 homogeneous model of 500  $\Omega$ -m half-space with a resistive block of 10000  $\Omega$ -m having a thickness of  
123 1 km was embedded in the model from surface relief (Fig. 1). The MT responses for the model have  
124 been computed with and without topography. The terrain correction procedures (TCP1 & TCP2) have

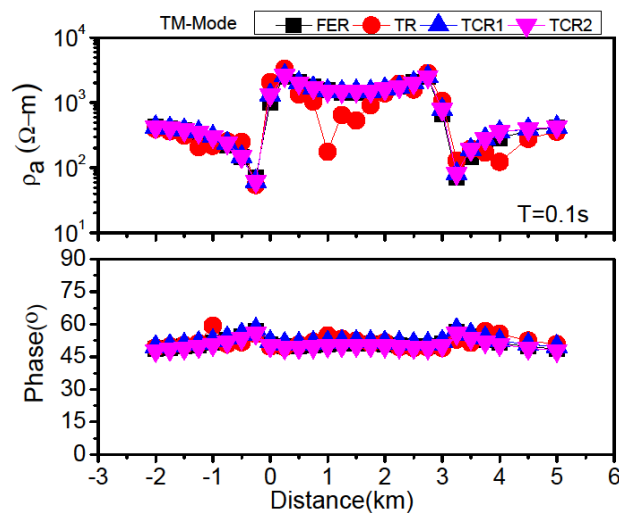


125 been applied to the model responses at a particular period of 0.1 second (sec) and validated over the  
126 inhomogeneous model of Chouteau and Bouchard (1988). In 2D the topography effect is galvanic in  
127 TM mode and inductive in TE mode. Therefore, the comparison of TM component of flat earth  
128 response (FER), topographic response (TR) and two terrain correction responses (TCR1 and TCR2)  
129 were shown in Fig. 2. It is concluded from the Fig. 2 that the TCR1 and TCR2 are very similar to the  
130 FER at particular period of 0.1 sec, but not similar to the TR, which shows a good agreement of  
131 published result of Chouteau and Bouchard (1988).



132

133 **Fig. 1:** Topographic model of  $500 \Omega\text{-m}$  half-space with a resistive body of  $10000 \Omega\text{-m}$  was embedded  
134 from the surface relief (Chouteau and Bouchard, 1988).

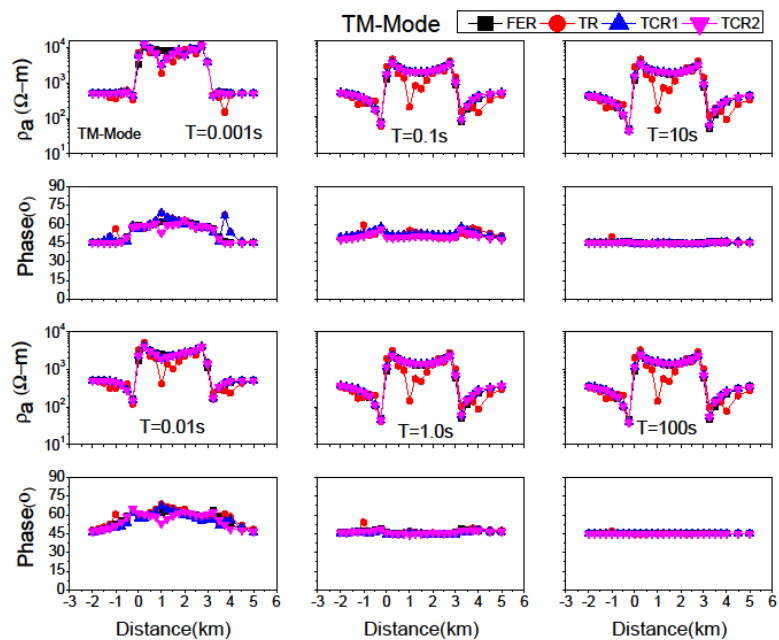


135

136 **Fig. 2:** Comparison of TM component of flat earth response (FER), topographic response (TR) and  
137 two terrain correction responses (TCR1 and TCR2) at 0.1 sec.

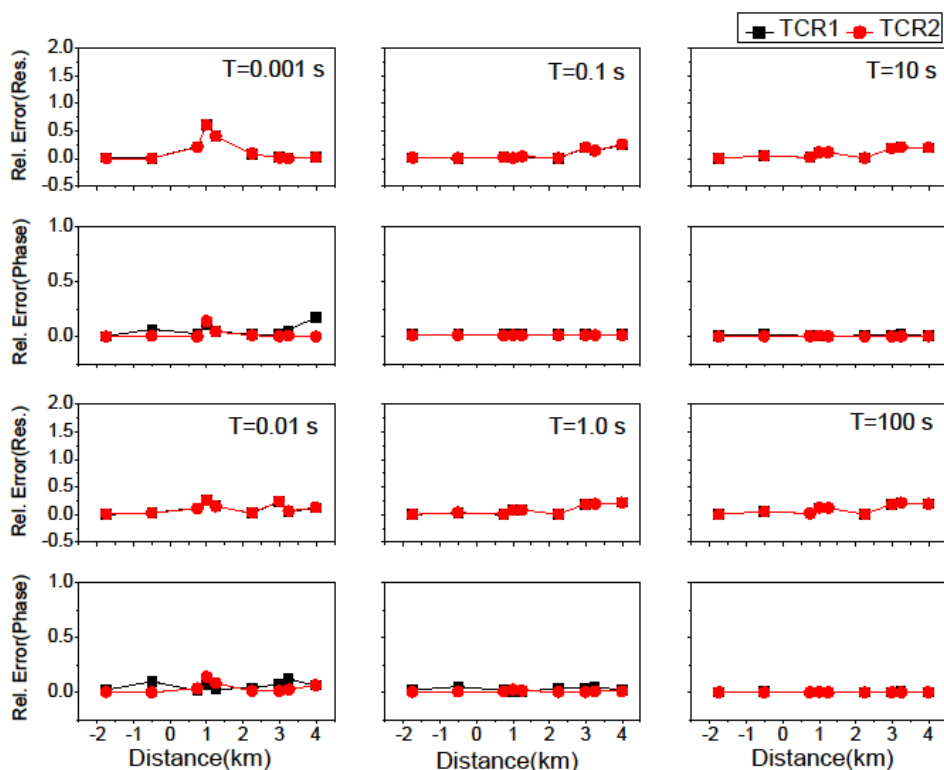
138 Fig. 3 showed that the topography distortions are large for higher period in apparent resistivity  
139 component only, which shows the galvanic nature of the topography distortions. The terrain corrected  
140 responses (TCR1 and TCR2) in Fig. 3 are almost similar to flat earth responses (FER) at six periods  
141 (0.001 sec, 0.01 sec, 0.1 sec, 1 sec, 10 sec, and 100 sec respectively). Relative errors were also  
142 calculated to check the accuracy of the terrain correction responses (TCR1 and TCR2) with flat earth  
143 responses at these periods. The relative error between the FER and TCR1 and TCR2 were very small  
144 at all these periods except at site D only at lower periods (because of 10000 Ω-m resistive body) as  
145 shown in Fig. 4. This shows the accuracy of the correction procedures.





146

147 **Fig. 3:** Comparison of TM components of flat earth response (FER), topographic response (TR), and  
148 two correction procedures (TCR1 and TCR2) for the model in Fig. 1 at six different periods (0.001  
149 sec, 0.01 sec, 0.1 sec, 1sec, 10 sec and 100 sec).



150

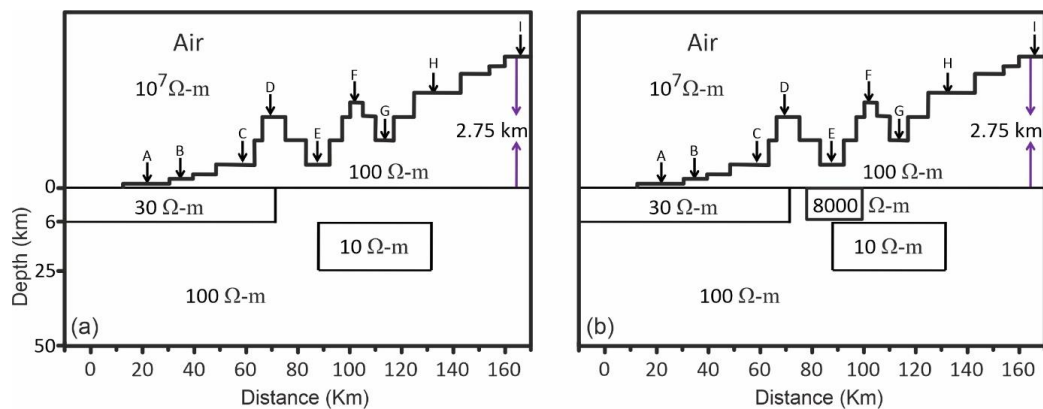
151 **Fig. 4:** Relative error between terrains corrected responses (TCR1 and TCR2) with respect to flat  
152 earth responses (apparent resistivity and phase) at six different periods with homogeneous half-space  
153 of 500  $\Omega$ -m resistivity.

#### 154 **4. MODELING OF ROORKEE TO GANGOTRI SECTION:**

155 A theoretical analysis of the effect of topography on MT responses was also taken into account in the  
156 Himalayan topography model. A theoretical model of Roorkee-Gangotri Profile was generated to  
157 simulate the MT response. To compute the MT forward modeling responses over the rugged  
158 topographic surface in Roorkee to Gangotri section, the input model was prepared from a 2D inverted  
159 geoelectrical resistivity model (Tyagi, 2007).The topography model having an elevation of 2.75 km



160 consists of a 180 km long profile from Roorkee to Gangotri drawn (Tyagi, 2007; Suman et al.,  
161 2023). In this model, two conductive blocks having resistivity  $30 \Omega\text{-m}$  and  $10 \Omega\text{-m}$  were embedded in  
162 a homogeneous half-space of  $100 \Omega\text{-m}$  resistivity. The first block of resistivity  $30 \Omega\text{-m}$  having width  
163 80 km and thickness 6 km was embedded just near the earth's surface relief and the second block of  
164 width 40 km and thickness 25 km was embedded at 6 km depth from the surface. The MT responses  
165 were computed by considering three models, (1) one with half-space of resistivity  $100 \Omega\text{-m}$  (Fig. 5a),  
166 (2) with half-space of resistivity  $500 \Omega\text{-m}$ , (3) with an additional resistive body of  $8000 \Omega\text{-m}$   
167 embedded from earth surface relief having thickness about 6 km with half-space of resistivity  $100 \Omega\text{-m}$   
168 m as shown in Fig. 5b. The topography response (TR), flat earth response (FER) and two topography  
169 corrected responses (TCR1 & TCR2) were analysed for nine sites (A, B, C, D, E, F, G, H & I) as  
170 shown in Fig. 5 at six distinct periods (0.00131 sec, 0.0102 sec, 0.1063 sec, 1.1110 sec, 11.6078 sec,  
171 and 121.2813 sec).



172

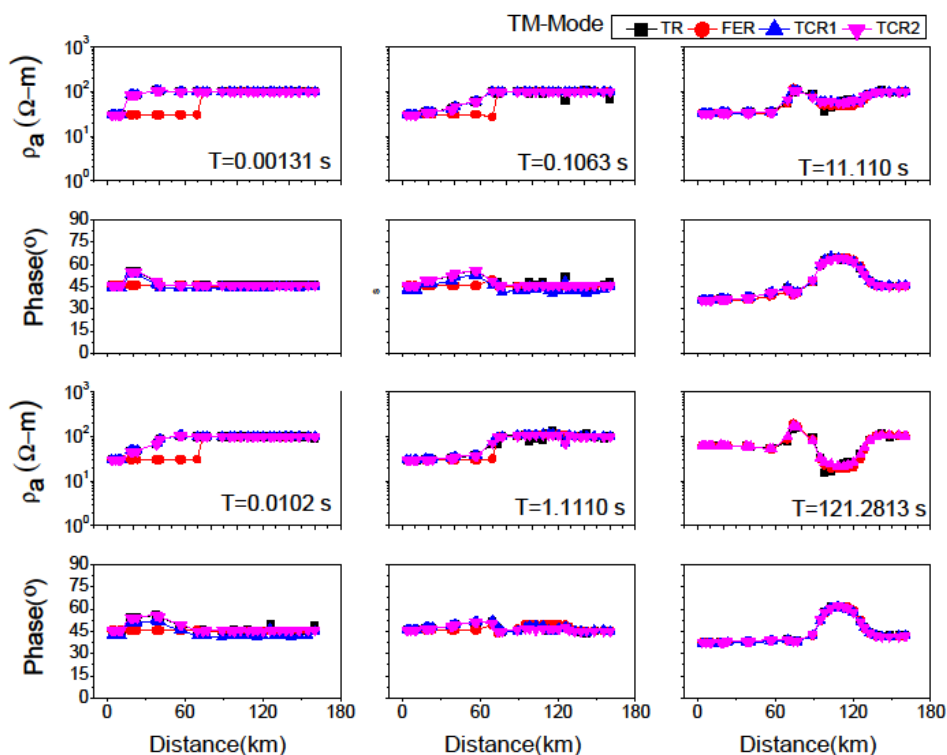
173 **Fig. 5:** (a) A Synthetic model of Garhwal Himalaya along Roorkee to Gangotri Profile in half-space of  
174 resistivity  $100 \Omega\text{-m}$  (b) with a resistive block of resistivity  $8000 \Omega\text{-m}$ .

## 175 5. RESULT AND DISCUSSION:

### 176 5.1. Model with half-space of resistivity $100 \Omega\text{-m}$ :



177 The topography response (TR) and flat earth response (FER) were computed for the topography  
178 model with a conductive body of 30  $\Omega$ -m resistivity in a half-space of 100  $\Omega$ -m resistivity (Fig. 5a) and  
179 the topography corrections procedures were applied to the MT data. Fig. 6 shows the TM mode of  
180 topography response (TR), flat earth response (FER) and two topography correction responses (TCR1  
181 & TCR2) at six different periods (0.00131 sec, 0.0102 sec, 0.1063 sec, 1.1110 sec, 11.6078 sec, and  
182 121.2813 sec). The topography effect depends upon the ramp/slope angle of the hill and is significant  
183 when the slope angle is greater than  $7.5^\circ$  (Kumar et al., 2018). It is clear from Fig. 6 that the TCR1  
184 and TCR2 are almost similar to the topographic response, because the slope angle is less than  $1^\circ$ . The  
185 TCR1 & TCR2 were not similar to the flat earth response for the sites from A to D at lower periods  
186 0.00131 sec, 0.0102 sec, 0.1063 sec and 1.111 sec, because of the exposure of the conductive body  
187 having resistivity 30  $\Omega$ -m to the surface (from A to D) and its galvanic effect. The relative errors were  
188 also calculated between the FER with TCR1 and TCR2 and were high for the sites A, B and C for  
189 lower periods (0.00131sec, 0.0102 sec and 0.10631 sec) due to the presence of the conductive body  
190 underneath these sites and was very small for all other sites D, E, F, G, H and I at all periods as shown  
191 in Fig. 7.

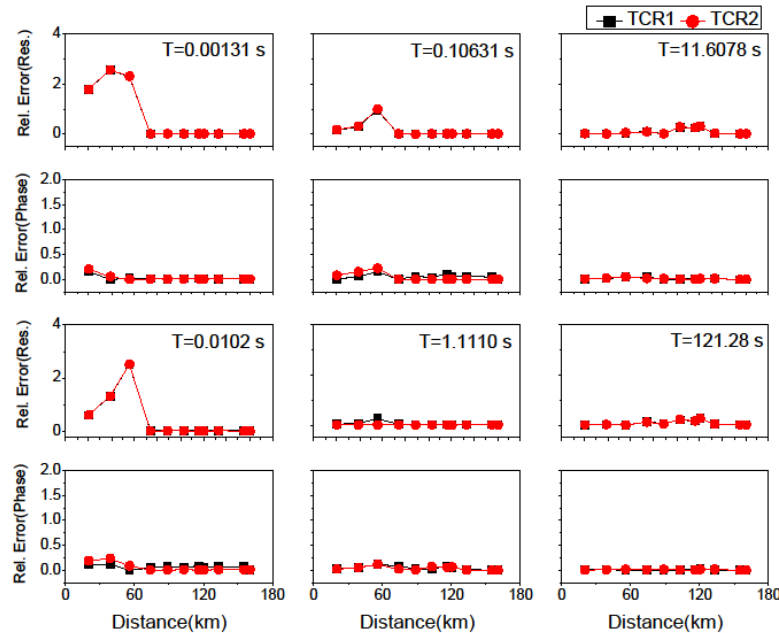


192

193 **Fig. 6:** Comparison of TM components of flat earth response (FER), topographic response (TR), and

194 two correction procedures (TCR1 and TCR2) at six different periods for homogeneous half-space of

195 resistivity 100 Ω-m.

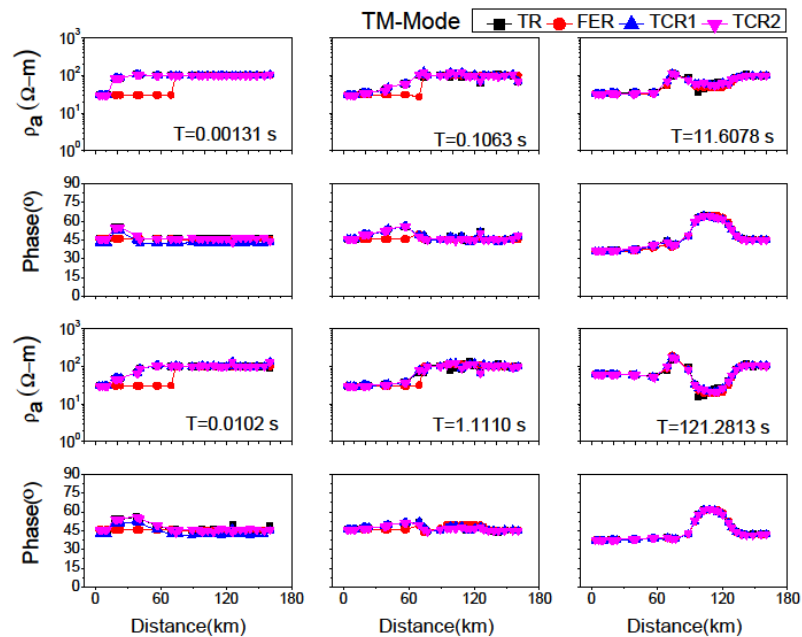


196

197 **Fig. 7:** Relative error between terrains corrected responses (TCR1 and TCR2) with respect to flat  
198 earth response (apparent resistivity and phase) at six different periods with half-space of resistivity  
199 100  $\Omega$ -m.

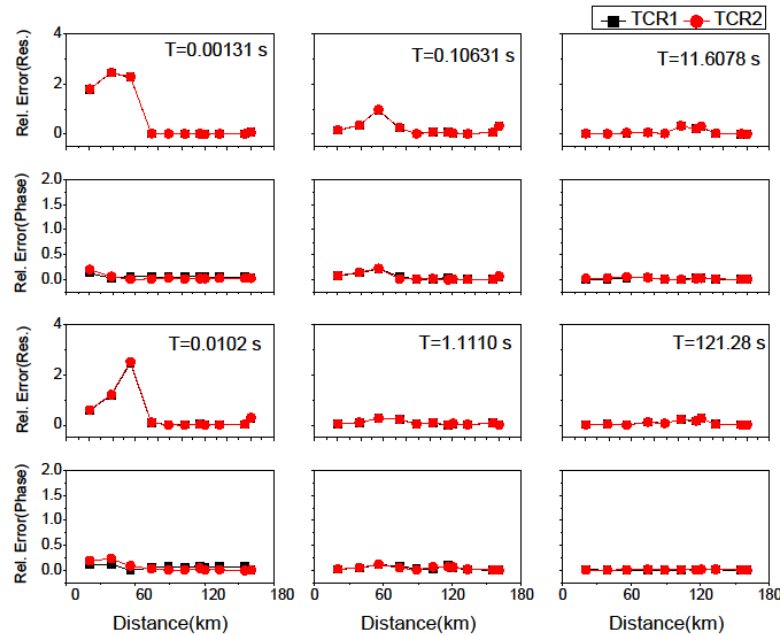
### 200 **5.2. Model with half-space of resistivity 500 $\Omega$ -m:**

201 Now consider the case in which model half-space resistivity was replaced with 500  $\Omega$ -m in Fig. 5a.  
202 The topography response (TR) and flat earth response (FER) were computed for the topography  
203 model with half-space of 500  $\Omega$ -m resistivity (Fig. 5a) and the topography correction procedures were  
204 applied to the MT data. Fig. 8 shows the TM component of topography response (TR), flat earth  
205 response (FER), and topography corrected responses (TCR1 & TCR 2) at six different periods. The  
206 results were almost similar to the response of the model with half-space of resistivity 100  $\Omega$ -m. The  
207 relative errors were also calculated in this case also between the FER with TCR1 and TCR2 and the  
208 results were similar to the model with half-space of 100  $\Omega$ -m at all these periods (0.00131 sec, 0.0102  
209 sec, 0.1063 sec, 1.1110 sec, 11.6078 sec, and 121.2813 sec) as shown in Fig. 9.



210

211 **Fig. 8:** Comparison of TM components of flat earth response (FER), topographic response (TR), and  
212 two correction procedures (TCR1 and TCR2) at six different periods for half-space of resistivity 500  
213  $\Omega$ -m.



214

215 **Fig. 9:** Relative error between terrains corrected responses (TCR1 and TCR2) with respect to flat  
216 earth response (apparent resistivity and phase) at six different periods with half-space of resistivity  
217 500  $\Omega$ -m.

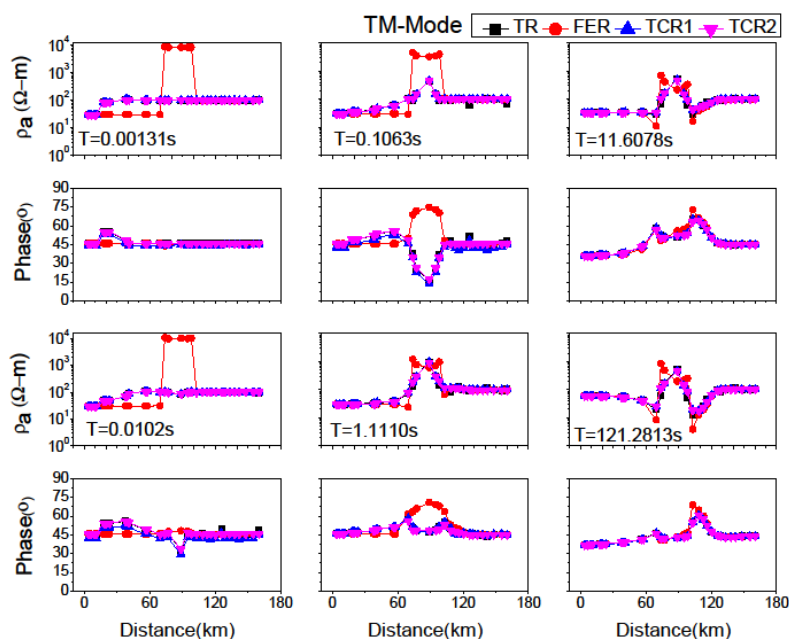
218 **5.3. Model with a resistive block of resistivity 8000  $\Omega$ -m in half-space of 100 $\Omega$ -m:**

219 The topography response (TR) and flat earth response (FER) were also computed for the topography  
220 model with a resistive block of resistivity 8000  $\Omega$ -m in half-space of 100  $\Omega$ -m resistivity (Fig. 5b) and  
221 the topography corrections were applied to the MT data. Fig. 10 shows the TM component of  
222 topography response (TR), flat earth response (FER) and two topography correction responses (TCR1  
223 & TCR2) at six different periods. The TCR1 & TCR2 were not similar to the flat earth model for the  
224 sites from A to F, because of the exposure of the conductive body having resistivity 30  $\Omega$ -m to the  
225 surface (from A to D) and its galvanic effect and the presence of 8000  $\Omega$ -m resistive body (from D to





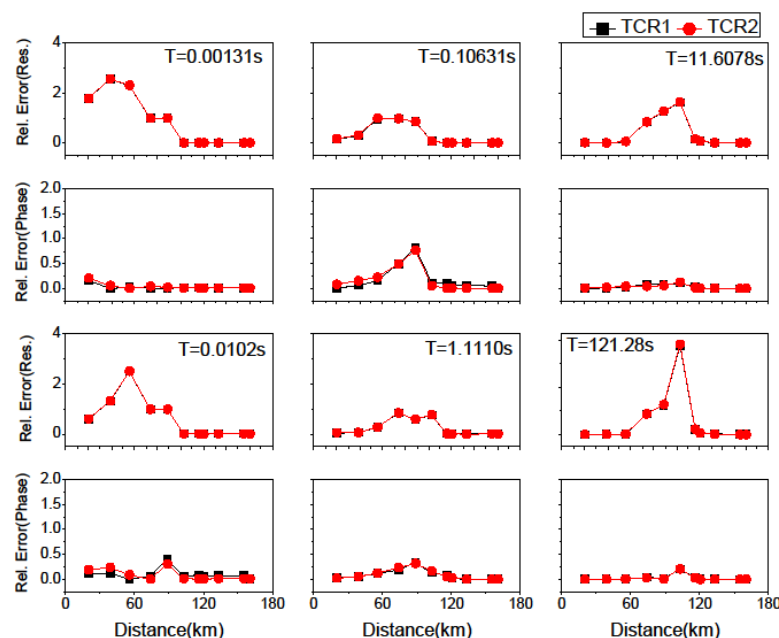
226 F). The relative errors were also calculated between the FER with TCR1 and TCR2 and were high for  
 227 the sites A, B and C for lower periods (0.00131 sec, 0.0102 sec and 0.10631 sec) due to the presence  
 228 of the conductive body underneath these sites and for higher periods (1.1110 sec, 11.6078 sec and  
 229 121.2813 sec) the relative error was again high due the presence of the 8000 Ω-m resistive body from  
 230 D to F as shown in Fig. 11.



231

232 **Fig. 10:** Comparison of TM components of flat earth response (FER), topographic response (TR), and  
 233 two correction procedures (TCR1 and TCR2) at six different periods for half-space of resistivity 100  
 234 Ω-m.

235



236

237 **Fig. 11:** Relative error between terrains corrected responses (TCR1 and TCR2) with respect to flat  
 238 earth response (apparent resistivity and phase) at six different periods with half-space of resistivity  
 239 100  $\Omega$ -m.

240 **6. CONCLUSIONS:**

241 The study shows the effect of topography in the MT data along a synthetic model of Roorkee-  
 242 Gangotri profile. The two correction procedures were used to remove the topography distortion from  
 243 MT data. The similar FER, TCR1 and TCR2 in Fig. 3 shows that the both correction procedures are  
 244 capable to remove the topography effect, this shows the efficacy of the two correction procedures. The  
 245 similar TR, TCR1 and TCR2 responses (Fig. 6, 8 and 10) concluded that there is no need for  
 246 topography correction along Roorkee-Gangotri Profile, because the slope angle is less than one  
 247 degree. The relative error between the FER and TCR1 and TCR2 also showed the accuracy of the two



248 correction procedures (TCR1 & TCR2) in this study. The presence of near surface  
249 heterogeneity/surface exposure of conductive/resistive body also distort the MT responses as in this  
250 model (the FER not similar to TR, TCR1 and TCR2).

## 251 **ACKNOWLEDGEMENT**

252 Suman thank Head of Department, Department of Physics, M. M. Engineering College, Maharishi  
253 Markandeshwar (Deemed to be) University for continuous guidance and support throughout this  
254 research.

## 255 **AUTHOR CONTRIBUTION:**

256 Dr. Deepak Kumar Tyagi and Ms Suman Saini designed the experiments, developed the model  
257 and performed the simulations. Dr Rajeev Sehrawat, Dr. Sushil Kumar prepared the manuscript  
258 with contributions from all the co-authors.

## 259 **COMPETING INTERESTS**

260 The authors declare that they have no conflict of interest.

## 261 **REFERENCES**

- 262 1. Cagniard, L.: Basic theory of the magneto-telluric method of geophysical prospecting.  
263 Geophysics. **18** 605-635, 1953.
- 264 2. Changhong, Lin.: The effects of 3D topography on controlled-source audio-frequency  
265 magnetotelluric responses. Geophysics. **83** no. 2 p. Wb97–wb108, 1910.1190/geo-0429, 2018.
- 266 3. Chouteau, M., and Bouchard, K.: Two-dimensional terrain correction in magnetotelluric. Surveys  
267 Geophysics. **53** 854-862, 1988.
- 268 4. Coggon, H.: Electromagnetic and electrical modeling by the finite-element method: Geophysics.  
269 **36** 132-155, 1971.



- 270 5. Faradzhev, A. S., Kakhramanov, K. K., Sarkisov, G. A., and Khalilova, N. E.: On effects of  
271 terrain on magnetotelluric sounding (MTS) and profiling (MTP). *Izvestia Earth Physics*. **5** 329-  
272 330, 1972.
- 273 6. Franke, A., Börner, R. U., and Spitzer, K.: Adaptive unstructured grid finite element simulation of  
274 two-dimensional magnetotelluric fields for arbitrary surface and seafloor topography.  
275 *Geophysical Journal International*. **171** 71-86, 2007.
- 276 7. Gurer, A., and Ilkisik, M.: The importance of topographic corrections on magnetotelluric response  
277 data from rugged regions of Anatolia, *Geophys. Prospect*. **45** 111-125, 1997.
- 278 8. Harinarayana, T., and Sarma, S. V. S.: Topographic effects on telluric field measurements.  
279 *Pageoph*. **120** 778-783, 1982.
- 280 9. Holcombe, H. T., and Jiracek, G. R.: 1984 Three-dimensional terrain corrections in resistivity  
281 surveys: *Geophysics*. **49** 439-452, 1977.
- 282 10. Israil, M., Tyagi, D. K., Gupta, P. K., and Niwas, Sri.: Magnetotelluric investigations for imaging  
283 electrical structure of Garhwal Himalaya corridor, Uttarakhand, India. *Journal of Earth System*  
284 *Sci.* **117** 189-200, 2008.
- 285 11. Israil, M., Mamoriya, P., Gupta, P. K., and Varshney, S. K.: Transverse Tectonics Feature  
286 Delineated by Modelling of Magnetotelluric Data from Garhwal Himalaya Corridor, India. *Curr.*  
287 *Sci.* **111** 868-875, 2016.
- 288 12. Jiracek, G. R., Redding, R. P., and Kojima, R. K.: Application of the Rayleigh-FFT technique to  
289 magnetotelluric modeling and correction. *Physics of the Earth and Planetary Interiors*, **53** 365-  
290 375, 1989.
- 291 13. Jiracek, G.: Near-surface and topographic distortions in electromagnetic induction. *Surveys*  
292 *Geophysics*. **11** 163-203, 1990.
- 293 14. Konda, S., Patro, P. K., Reddy, K. C., and Babu, N.: Three-dimensional magnetotelluric  
294 signatures and rheology of subducting continental crust: Insights from Sikkim Himalaya, India.  
295 *Journal of Geodynamics*. **155** 101961, 2023.
- 296 15. Ku, C. C., Hsieh, M. S., and Lim, S. H.: The topographic effect in electromagnetic fields. *Can. J.*  
297 *Earth Sci.* **10** 645-656, 1973.
- 298 16. Kumar, D., Singh, A., and Israil, M.: Necessity of Terrain Correction in Magnetotelluric Data  
299 Recorded from Garhwal Himalayan Region, India. *Geosciences*. **11** 482, 2021.



- 300 17. Kumar, G. P., Manglik, A., and Thiagarajan, S.: Crustal Geoelectric Structure of the Sikkim  
301 Himalaya and Adjoining Gangetic Foreland Basin. *Tech. physics.* **637** 238-250, 2014.
- 302 18. Kumar, S., Patro, P. K., and Chaudhary, B. S.: Three dimensional topography correction applied  
303 to magnetotelluric data from Sikkim Himalayas. *Physics Earth Planet. Int.* **279** 33-46, 2018.
- 304 19. Kumar, S., Patro, K. P., and Chaudhary, B. S.: Subsurface Resistivity Image of Sikkim Himalaya  
305 as Derived from Topography Corrected Magnetotelluric Data. *Journal of the Geological Society*  
306 *of India.* DOI: 10.1007/s12594-022-1985-2, 2022.
- 307 20. Larsen, J. C.: Removal of local surface conductivity effects from low frequency mantle response  
308 curves, *ActaGeodaet., Geophys. et Montanist. Acad. Sci. Hung. Tomus.* **12** (1-3) 183-186, 1977.
- 309 21. Mohan, K., Kumar, G. P., Chaudhary, P., Choudhary, V. K., Nagar, M., Khuswaha, D., Patel, P.,  
310 Gandhi, D., and Rastogi, B. K.: Magnetotelluric Investigations to Identify Geothermal Source  
311 Zone near Chabsar Hotwater Spring Site, Ahmedabad, Gujarat, Northwest India. *Geothermics.*  
312 **65** 198-209, 2017.
- 313 22. Nam, M. J., Kim, H. J., Song, Y., Lee, T. J., Son, J. S., and Suh, J. H.: Three-dimensional  
314 topography corrections of magnetotelluric data. *Geophysics J. Int.* **174** 464-474, 2008.
- 315 23. Ngoc, P. V.: Magnetotelluric survey of the Mount Meager region of the Squamish Valley (British  
316 Columbia). *Geomagnetic Service of Canada, Earth Physics Branch of the Dept. of Energy,*  
317 *Mines and Resources of Canada.* Rep. 80-8-E, 1980.
- 318 24. Patro, P. K., and Harinarayana, T.: Deep Geoelectric Structure of the Sikkim Himalayas (NE  
319 India) Using Magnetotelluric Studies. *Phys. Earth Planet. Inter.* **173** 171-176, 2009.
- 320 25. Patro, P. K.: Magnetotelluric Studies for Hydrocarbon and Geothermal Resources: Examples  
321 from the Asian Region. *Surveys Geophysics.* **38** 1005-1041, 2017.
- 322 26. Rastogi, A.: A finite difference algorithm for two-dimensional inversion of geo-  
323 electromagnetic data. Ph. D. Thesis, University of Roorkee (India), 1997.
- 324 27. Rijo, L.: Modelling of electric and electromagnetic data: Ph.D. thesis, Univ. of Utah. **19**, 1977.
- 325 28. Suman, Tyagi, D. K., and Sherawat, R.: Topography distortion effect on Magnetotelluric (MT)  
326 profiling of Sub-Himalayan region using two-dimensional modelling. *J. Integr. Sci. Technol.* **11**  
327 462, 2023.
- 328 29. Thayer, R.E.: Topographic distortion of telluric currents: a simple calculation. *Geophysics.* **40** 91-  
329 95, 1975.



- 330 30. Tikhonov, A. N.: Determination of the Electrical Characteristics of the Deep Strata of the Earth's  
331 Crust. *DoklAkademiaNauk*. **73** 295-297, 1950.
- 332 31. Tyagi, D. K.: 2D modeling and inversion of magnetotelluric data acquired in Garhwal Himalaya,  
333 Ph. D. Thesis, 2007.
- 334 32. Vozoff, K.: The magnetotelluric method, in *Electromagnetic Methods in Applied Geophysics*.ed.  
335 Nabighian, M. N., Society of Exploration Geophysicists. **2** 641-711, 1991.
- 336 33. Wannamaker, P. E., Stodt, J. A., Rijo, L.: Two-dimensional topographic responses in  
337 magnetotellurics modeled using finite elements. *Geophysics*. **51** 2131-2144, 1986.
- 338 34. Ward, S. H., Peeples, W. J., and Ryu, J.: Analysis of geo-electromagnetic data: *Meth. Compo*  
339 *Phys*. **13** 163-238, 1973.
- 340 35. Wescott, E. M., and Hessler, V. P.: The effect of topography and geology on telluric currents.  
341 *Jour. Geophysics. Res*. **67** 4813-4823, 1962.
- 342 36. Xiong, B., Luo, T. Y., Chen, L. W., Dai, S. K., Xu, Z. F., Li, C. W., Ding, Y. L., Wang, H. H.,  
343 and Li, J. H.: Influence of Complex Topography on Magnetotelluric Observed Data Using  
344 Three-Dimensional Numerical Simulation: A Case from Guangxi Area, China. *Appl.*  
345 *Geophysics*. **17** 601-615, 2020.
- 346 37. Zhang, K., Wei, W., Lu, Q., Dong, H., and Li, Y.: Theoretical Assessment of 3-D Magnetotelluric  
347 Method for Oil and Gas Exploration: Synthetic Examples. *J. Appl. Geophysics*. **106** 23-36,  
348 2014.